The Journal of Immunology

A Novel Mechanism of Rapid Nuclear Neutrophil Extracellular Trap Formation in Response to *Staphylococcus aureus*

Florian H. Pilsczek, Davide Salina, Karen K. H. Poon, Candace Fahey, Bryan G. Yipp, Christopher D. Sibley, Stephen M. Robbins, Francis H. Y. Green, Mike G. Surette, Motoyuki Sugai, M. Gabriela Bowden, Muzaffar Hussain, Kunyan Zhang and Paul Kubes

J Immunol 2010; 185:7413-7425; Prepublished online 22 November 2010;
doi: 10.4049/jimmunol.1000675
http://www.jimmunol.org/content/185/12/7413

The Journal of Immunology is published twice each month by
The American Association of Immunologists, Inc.,
1451 Rockville Pike, Suite 650, Rockville, MD 20852

Print ISSN: 0022-1767 Online ISSN: 1550-6606.

A Novel Mechanism of Rapid Nuclear Neutrophil Extracellular Trap Formation in Response to *Staphylococcus aureus*

Florian H. Pilsczek,*,[1] Davide Salina,*,†,[1] Karen K. H. Poon,* Candace Fahey,* Bryan G. Yipp,* Christopher D. Sibley,*,‡ Stephen M. Robbins,§ Francis H. Y. Green,*,† Mike G. Surette,*,‡ Motoyuki Sugai,¶ M. Gabriela Bowden,‖ Muzaffar Hussain, Kunyan Zhang,†,‡ and Paul Kubes*,††**

Neutrophil extracellular traps (NETs) are webs of DNA covered with antimicrobial molecules that constitute a newly described killing mechanism in innate immune defense. Previous publications reported that NETs take up to 3–4 h to form via an oxidant-dependent event that requires lytic death of neutrophils. In this study, we describe neutrophils responding uniquely to *Staphylococcus aureus* via a novel process of NET formation that did not require neutrophil lysis or even breach of the plasma membrane. The multilobular nucleus rapidly became rounded and condensed. During this process, we observed the separation of the inner and outer nuclear membranes and budding of vesicles, and the separated membranes and vesicles were filled with nuclear DNA. The vesicles were extruded intact into the extracellular space where they ruptured, and the chromatin was released. This entire process occurred via a unique, very rapid (5–60 min), oxidant-independent mechanism. Mitochondrial DNA constituted very little if any of these NETs. They did have a limited amount of proteolytic activity and were able to kill *S. aureus*. With time, the nuclear envelope ruptured, and DNA filled the cytoplasm presumably for later lytic NET production, but this was distinct from the vesicular release mechanism. Panton–Valentine leukocidin, autolysin, and a lipase were identified in supernatants with NET-inducing activity, but Panton–Valentine leukocidin was the dominant NET inducer. We describe a new mechanism of NET release that is very rapid and contributes to trapping and killing of *S. aureus*. *The Journal of Immunology*, 2010, 185: 7413–7425.

Neutrophil extracellular traps (NETs) were discovered in 2004 and have been described as a potential bacterial killing mechanism. Brinkmann et al. (1) first reported that neutrophils were activated to release their DNA, which was laden with proteases that trapped and killed microbes. NETs have also been documented in vivo in several pathological conditions, including experimental shigellosis in rabbits and human appendicitis (1), preeclampsia (2), in the vasculature of a patient with acute interstitial pneumonitis (3), in skin lesions of patients with leishmaniasis (4), during autoimmune disease (5), and in pneumococcal pneumonia (6) and necrotizing fasciitis caused by *Streptococcus pyogenes* in mice (7–9). It is intriguing that numerous bacteria have evolved the ability to produce DNases, which recently have been shown to degrade NET components, thereby freeing themselves from capture (1, 6, 8). This increases the virulence of pathogens, such as *Streptococcus pneumoniae* (6) and *S. pyogenes* (7–9).

In a very detailed series of imaging experiments, Fuchs et al. (10) demonstrated that the formation of NETs in response to phorbol ester as well as *Staphylococcus aureus* is the last step in a process of active neutrophil death. These investigators showed that over the period of ~3 h, the neutrophils underwent very significant morphological changes dependent in part on the production of large quantities of oxidants from the neutrophil enzyme NADPH oxidase. NET formation was initiated by the loss of nuclear segregation of euchromatin and heterochromatin. The characteristic lobular form of the neutrophil nucleus was lost, and, at later time points, the nuclear envelope disintegrated. The granular membranes disappeared, and the nuclear, cytoplasmic, and granular components were mixed together. Finally, the cell membrane ruptured allowing the extrusion of the NETs. Importantly, in this form of cell death, DNA fragmentation did not occur, allowing the chromatin to unfold once released into the extracellular space. Fuchs et al. (10) concluded that this rather lengthy 3-h process of oxidant-dependent NET formation allowed neutrophils to continue their antimicrobial role even after cell death.

However, more recently, Yousefi et al. (11) reported that IL-5 or IFN-γ–primed eosinophils could catapult their DNA in response to LPS. This process was rapid and did not cause apoptosis of the eosinophils. The authors suggested that this was primarily

*Snyder Institute of Infection, Immunity and Inflammation, †Department of Pathology and Laboratory Medicine, ‡Department of Microbiology and Infectious Diseases, §Department of Oncology and Biochemistry and Molecular Biology, and ¶Department of Bacteriology, Hiroshima University, Hiroshima, Japan; ‖Center for Extracellular Matrix Biology, Texas A&M University System Health Science Center, Houston, TX 77030; **Institute of Medical Microbiology, University Hospital, Muenster, Germany; and ††Department of Physiology and Biophysics, University of Calgary, Calgary, Alberta T2N 4N1, Canada

[1]F.H.P. and D.S. contributed equally to this work.

Received for publication February 26, 2010. Accepted for publication October 7, 2010.

F.H.P. is an Alberta Heritage Foundation for Medical Research clinical research fellowship award holder, and P.K., S.M.R., and M.G.S. are Alberta Heritage Foundation for Medical Research scientists.

Address correspondence and reprint requests to Dr. Paul Kubes, Immunology Research Group, Department of Physiology and Biophysics, University of Calgary, 3280 Hospital Drive N.W., Calgary, AB, T2N 4N1, Canada. E-mail address: pkubes@ucalgary.ca

The online version of this article contains supplemental material.

Abbreviations used in this paper: DPI, dibenziodolium chloride; INM, inner nuclear membrane; LDH, lactate dehydrogenase; MS/MS, tandem mass spectrometry; NET, neutrophil extracellular trap; NPC, nuclear pore complex; ONM, outer nuclear membrane; PVL, Panton–Valentine leukocidin; ROS, reactive oxygen species.

www.jimmunol.org/cgi/doi/10.4049/jimmunol.1000675

due to the fact that eosinophils extruded mitochondrial not nuclear DNA. The same group also reported that neutrophils, primed with GM-CSF, would then respond to LPS or C5a by releasing mitochondrial DNA via an oxidant-mediated event (12). In this way, a neutrophil could release NETs but retain its nucleus and presumably continue its other antimicrobial functions. However, neutrophils are terminally differentiated cells that do not need protein synthesis to survive for their very short life span and perform their effector functions. Indeed, the nucleus and constituent DNA were demonstrated to be expendable decades ago. Vigorous spinning of neutrophils to remove nuclei rendered anuclear, resealed cytoplasts that had the capacity to chemotax, phagocytose, and kill bacteria (13) raising the possibility that a neutrophil might be able to survive even if it released its nuclear DNA.

S. aureus is one of the most common human pathogens responsible for more than 10 million skin and soft tissue infections each year in North America alone (14). *S. aureus* has evolved multiple mechanisms of inhibiting neutrophil phagocytosis by interfering with complement activation and preventing Fc receptor binding to Ab immobilized to *S. aureus* (15–18). Even if *S. aureus* is phagocytosed, it can survive inside neutrophils (19). Therefore, a rapid extracellular killing mechanism might be a more effective strategy to eradicate *S. aureus*. In this study, we identified that neutrophils employ a very rapid novel process of nuclear NET formation primarily in response to *S. aureus* that is distinct from the previously reported NET formation inasmuch as it does not require oxidant-dependent processes, neutrophil lysis, or mitochondrial DNA release.

Materials and Methods

Reagents and media

Unless stated otherwise, all reagents were purchased from Sigma Chemical Company (St. Louis, MO). Bacteria were grown on Todd–Hewitt agar supplemented with 5% yeast and in brain heart infusion broth at 37°C and 5% carbon dioxide. All culture media for bacteria were purchased from Difco (Sparks, MD) unless stated otherwise. DMEM was purchased from Difco and prepared according to the protocol of the manufacturer.

Bacterial strains and culture conditions

Escherichia coli was grown on Lenox L agar plates and in Luria broth (Invitrogen, Carlsbad, CA). *S. pneumoniae* was grown on Columbia agar supplemented with 5% sheep blood. *S. aureus* was grown on tryptic soy and brain heart infusion agar. The following bacteria were used in this study: *S. aureus* ATCC 25923; *Staphylococcus epidermidis* ATCC 14990; *Pseudomonas aeruginosa* PA01; *Gemella haemolysans* C304 (cultivated from sputum of a cystic fibrosis patient and identified with 16S rRNA sequencing); *S. pyogenes* ATCC 19615; *S. pneumoniae* ATCC 6303; *Acinetobacter baumannii* ATCC 19761; *E. coli* #16/126075 (cultivated by Calgary Laboratory Services [Calgary, Alberta, Canada] from blood of a patient with sepsis). In some cases, bacteria were lysed as previously described (20). In addition, we also used the following clinical strains of *S. aureus*: USA 400 (C8830) was obtained from a patient with serious skin infection, and M92 was a nasal colonizing strain obtained from a healthy individual. The lipase nonsecreting strain of *S. aureus* (MW2 geh::psk950) and the parent strain were used as described (21).

Human neutrophil isolation

Whole blood was collected into acid citrate dextrose (1:5 blood, v/v). Erythrocytes were removed using dextran sedimentation followed by two rounds of hypotonic lysis. Neutrophils were isolated from the resulting cell suspension using Ficoll-Histopaque density centrifugation. Purified neutrophils were suspended in DMEM at a concentration of 1×10^7 cells/ml (3).

Ethics statement

Permission for taking blood samples from human donors was obtained from the Foothills Hospital (Calgary, Alberta, Canada) ethics board. Written informed consent was provided by each human subject who donated blood.

NETs quantification assay

S. aureus were grown to stationary phase for 20 h, centrifuged for 2 min at 20,000 × *g*, and the pellet resuspended in normal saline. Bacteria were quantified as previously described (20). Bacteria were added to neutrophils in DMEM in 1.5-ml tubes at bacteria to neutrophil ratios of 10:1 (determined from preliminary work) and incubated at 37°C and 5% carbon dioxide for various times. PMA, a potent inducer of NET production (1) and a protein kinase C activator of neutrophils, was used at 20 nM or 100 μM. Sytox Green (Molecular Probes, Carlsbad, CA) was used in 96-well culture plates at 2.5 μM and studied with a 1420 Multilabel Counter Victor 3V fluorescence reader (PerkinElmer, Waltham, MA). Fluorescence was due to extracellular DNA as addition of DNase abolished fluorescence.

Microscopy

In some experiments, a Richardson RTM-3 microscope (Richardson Technologies, Bolton, Ontario, Canada) was used. The percentage of total surface area covered by NETs was determined with ImageJ software version 1.41 (National Institutes of Health, Bethesda, MD). In some experiments, NETs were visualized using autologous plasma-coated culture dishes (35 mm; World Precision, Sarasota, FL) and a confocal microscope (Olympus, Center Valley, PA, IX81 inverted confocal microscope with Fluoview 1000 acquisition software, ×40 objective). In some experiments, a cell-impermeable membrane culture insert (0.02 μm, 25 mm; Nunc, Rochester, NY) was used for separation of neutrophils and *S. aureus*. Sytox Green (5 μM), Hoechst 33342 (5 μg/ml), and propidium iodide (5 μg/ml) were purchased from Molecular Probes.

Cytotoxicity assay

Lysis of neutrophils was studied with the lactate dehydrogenase detection assay CytoTox-ONE Homogeneous Membrane Integrity Assay (Promega, Madison, WI) according to the protocol of the manufacturer. Fluorescence was detected with a fluorescence reader (PerkinElmer Fusion with Fusion Instrument Control Application 4.0).

Viability of neutrophils

Viability of neutrophils was tested with the Live/Dead Fixable Red Dead Cell Stain kit (Invitrogen), and apoptosis of neutrophils was tested with the APO-BrdU TUNEL assay kit (Invitrogen) according to the protocols of the manufacturer. A FACScan flow cytometer and CellQuest Pro software from BD Biosciences (Sparks, MD) were used.

Elastase assay

The EnzChek elastase assay kit (Molecular Probes) was used according to the protocol of the manufacturer. Fluorescence was detected with an X4 2030 Multilabel Reader fluorescence reader (PerkinElmer).

Reactive oxygen substrate assay

To quantify ROS, cytochrome c reduction was detected with increase of absorbance at 550 nm (extinction coefficient = 21.1 cm^{-1} mM^{-1}) with a spectrophotometer (Biomate-3; Thermo Spectronic, Burlington, Ontario, Canada) as part of a standard cytochrome c reduction assay. Cu/Zn superoxide dismutase (300 UN per ml; Oxis, Foster City, CA and Sigma, St. Louis, MO), which metabolizes reactive oxygen species (ROS), and diben-ziodolium chloride (DPI; 10–250 μM; Sigma), an inhibitor of NADPH oxidase, were used to confirm that reactive oxygen substrates were detected.

Scanning electron microscopy

Coverslips were coated with autologous plasma and incubated for 1 h at 37°C and 5% carbon dioxide. Neutrophils and *S. aureus* were prepared as before but incubated on coverslips. The incubated cells were fixed with 2.5% glutaraldehyde, postfixed with 1% osmium tetroxide/1% tannic acid, dehydrated with a graded ethanol series, critical-point dried, and covered with a gold film by sputter coating. The specimens were analyzed with an FEI XL30 ESEM (Hillsboro, OR) scanning electron microscope.

Transmission electron microscopy

Neutrophils and *S. aureus* were prepared as before and fixed with 2.5% glutaraldehyde. The supernatant was removed and warm 2% agar added. After cooling the embedded pellet was cut into pieces. After washing three times, the pieces were postfixed in 1% osmium tetroxide in cacodylate buffer for 1 h, dehydrated through a graded series of acetone, and embedded in epoxy-based resin. Ultrathin sections were cut in a Reichert-

Jung (Depew, NY) Ultracut E microtome using a diamond knife and stained with 4% aqueous uranyl acetate and Reynolds' lead citrate. The sections were observed in a Hitachi (Norcross, GA) H7650 transmission electron microscope at 80 kV, and images were taken with an AMT (Danvers, MA) 16000 digital camera mounted on the microscope.

Bacteria killing assay

Twenty-four–well culture plates were coated with 10% FBS (Hyclone, Burlington, Ontario, Canada) and subsequently washed three times with HBSS. *S. aureus* was grown to logarithmic phase, pelleted during centrifugation, suspended in normal saline, and incubated with autologous non-heat-inactivated serum at 10% for 30 min at room temperature. Neutrophils were prepared as before and resuspended in cold HBSS. Wells were filled with HBSS for a final volume of 500 μl. DNase was used at 5000 U per milliliter. After adding neutrophils, the culture plate was centrifuged at 200 × *g* for 5 min at room temperature and subsequently incubated at 37˚C and 5% carbon dioxide for 15 min. After incubation, bacteria were added to neutrophils at bacteria to neutrophil ratio of 10:1, and the culture plate was centrifuged as before followed by incubation at 37˚C and 5% carbon dioxide for 1 h. After incubation, 100-μl samples were obtained, serially diluted, plated, and grown overnight before counting of colonies.

Analysis of S. aureus *supernatant contents*

Brain heart infusion fluid media were inoculated with *S. aureus* ATCC 25923 and grown for 12 h at 37˚C and 250 rpm. The culture was used to inoculate 1:100 of 1 l brain heart infusion fluid media and grown for 12 h at 37˚C and 250 rpm. Supernatant was obtained by centrifugation at 20,000 × *g* for 20 min at 4˚C. Proteins were precipitated with 60% ammonium sulfate followed by centrifugation at 20,000 × *g* for 20 min at 4˚C. The precipitate was treated with desalting columns PD-10 followed by ion-exchange chromatography with HiTrap SP FF columns (both from GE Healthcare, Piscataway, NJ) and used according to the protocol of the manufacturer.

The collected fractions were tested for NET formation with the NET quantification assay, and fractions with activity were selected for further fractionation with gel filtration chromatography with Superose 6 columns (GE Healthcare) and used according to the protocol of the manufacturer. The collected fractions were tested for NET formation, and fractions inducing NETs were collected followed by one-dimensional SDS-PAGE. Individual bands were manually dissected and sent to the mass spectrometry facility.

In-gel destaining and digestion. Gel plugs were rinsed once with 200 μl HPLC-grade water, twice with 200 μl 25 mM ammonium bicarbonate in 50% (v/v) acetonitrile, followed by 100 μl acetonitrile to dehydrate the gel plugs, which were then lyophilized. The dry gel plugs were rehydrated in 5–7 μl 25 mM ammonium bicarbonate, pH 8, containing 12.5 ng/μl trypsin. After rehydration, an additional 30 μl 25 mM ammonium bicarbonate was added, and the gel plugs were incubated overnight at 37˚C. Peptides were extracted from gel plugs by two rounds of incubation with 50 μl 1% formic acid in 50% acetonitrile for 15 min. The pooled extracts were reduced to dryness and reconstituted in mobile phase buffer A for liquid chromatography.

Digests were analyzed using an integrated Agilent 1100 LC-Ion-Trap-XCT-Ultra system (Agilent Technologies, Santa Clara, CA), fitted with an integrated fluidic cartridge for peptide capture, separation, and nanospraying (HPLC Chip). Injected samples were trapped and desalted on a precolumn channel (40-nl volume; Zorbax [Palo Alto, CA] 300 SB-C_{18}) for 5 min with 3% acetonitrile with 0.2% formic acid delivered by an auxiliary pump at 4 μl/min. The peptides were then reverse-eluted from the trapping column and separated on the analytical column (150 mm length; Zorbax 300SB-C_{18}) at 0.3 μl/min. Peptides were eluted using a 5–70% (v/v) acetonitrile gradient in 0.2% (v/v) formic acid over 45 min. Tandem mass spectrometry (MS/MS) spectra were collected by data-dependent acquisition, with parent ion scans of 8100 Th/s over *m/z* 300–2000 and MS/MS scans at the same rate over *m/z* 100–2200. Peak-list data were extracted from these files by DataAnalysis software for the Agilent Technologies (Santa Clara, CA) 6300 series ion trap, v3.4 (build 175). Mascot v2.1 (Matrix Science, Boston, MA) was used to search the MS/MS data using the following parameters: 1.6 Da precursor ion mass tolerance, 0.8 Da fragment ion mass tolerance, one potential missed cleavage and oxidized methionine as a variable modification.

Specific S. aureus *reagents*

Recombinant autolysin was used as previously described by Dr. M. Sugai (Hiroshima University, Hiroshima, Japan). Purified LukF and LukS were provided by Dr. M. G. Bowden (Texas A&M University System Health Science Center, Houston, TX) after purification by ion-exchange chromatography followed by liquid chromatography (22). Antiserum from rabbits against amidase (60 kDa), glucosaminidase (50 kDa), the complete autolysin molecule (138 kDa, amidase and glucosamidase), and as control anti-epidermal differentiation factors A were used as previously described (23). Antiserum from rabbits against Panton–Valentine leukocidin (PVL)-F, PVL-S, PVL-FS, and as control plasmin sensitive IgG1 and clumping factor A IgG 1004 were used as previously described (24).

Statistical analysis

The unpaired one-tailed Student *t* test with a Bonferroni correction where necessary was used. A p value <0.05 was considered significant. For the electron microscopy counting, ANOVA was used to calculate the p value.

Results

S. aureus*: a unique NET inducer*

A wide variety of Gram-positive and Gram-negative bacteria were exposed to neutrophils, and rapid 1-h NET formation was quantified by measuring DNA content with Sytox Green, a molecule that is fluorescent when it intercalates into strands of DNA (25) but is impermeant to live cells. DNase was used to ensure DNA specificity. NET structures were confirmed using three different microscopy techniques. Neutrophils alone released very little DNA into the surrounding milieu consistent with the fact that the freshly isolated neutrophils were quiescent (Fig. 1*A*). Most Gram-negative or Gram-positive bacteria induced a 2- to 3-fold increase in extracellular DNA in 1 h (Fig. 1*A*). In dramatic contrast, *S. aureus* induced more than 10-fold NETs within a 1-h incubation period (Fig. 1*A*). Micrococcal nuclease is an enzyme found in *S. aureus* that has previously been shown to increase the NET signal with Sytox Green. To ensure this was not why the signal was so much higher in *S. aureus*, we added micrococcal nuclease (from *S. aureus*) to other strains of bacteria. This had no effect on our readout at lower concentrations and decreased the signal at higher concentrations (data not shown) suggesting that our *S. aureus* results may actually underestimate the amount of NETs formed.

S. pyogenes and *P. aeruginosa* also induced a substantial amount of extracellular DNA. DNase added 10 min before the end of the 1-h incubation (Fig. 1*A*) eliminated Sytox Green fluorescence. When cells were sonicated, over 10- to 20-fold more DNA was detected than that under control conditions (data not shown). PMA, at a concentration used by others (20 nM) (10) as a potent inducer of NETs over 3–4 h, caused almost no DNA release during the first hour of neutrophil stimulation (data not shown) consistent with previous reports (1). A much higher dose of PMA (100 μM), known to induce apoptosis (26), caused only a small release of extracellular DNA (Fig. 1*A*).

Sytox Green could potentially intercalate into extracellular bacterial DNA. However, only *P. aeruginosa* released significant amounts of its own DNA in the absence of neutrophils (Supplemental Fig. 1*A*). When bacteria were lysed, again only *P. aeruginosa* had significant DNA content (Supplemental Fig. 1*B*). Most importantly, the extracellular DNA was not secondary to lysis of neutrophils, despite *S. aureus* having lytic properties (15). An insignificant change in lactate dehydrogenase (LDH), a marker of cell lysis, was observed from neutrophils exposed to *S. aureus* or any of the other bacteria examined. Therefore, lysis could not account for the dramatic increase in DNA release with *S. aureus.* When very high doses of PMA (100 μM) were used, a small amount of DNA was deected, but LDH also increased (Fig. 1*B*). LDH increased 10-fold when neutrophils were lysed with Triton X-100 (Fig. 1*B* and Supplemental Fig. 1*C*).

We used a wide range of *S. aureus* to neutrophil ratios and observed optimal NET production (Supplemental Fig. 2*A*) and minimal LDH release (Supplemental Fig. 2*B*) at a ratio of 10:1

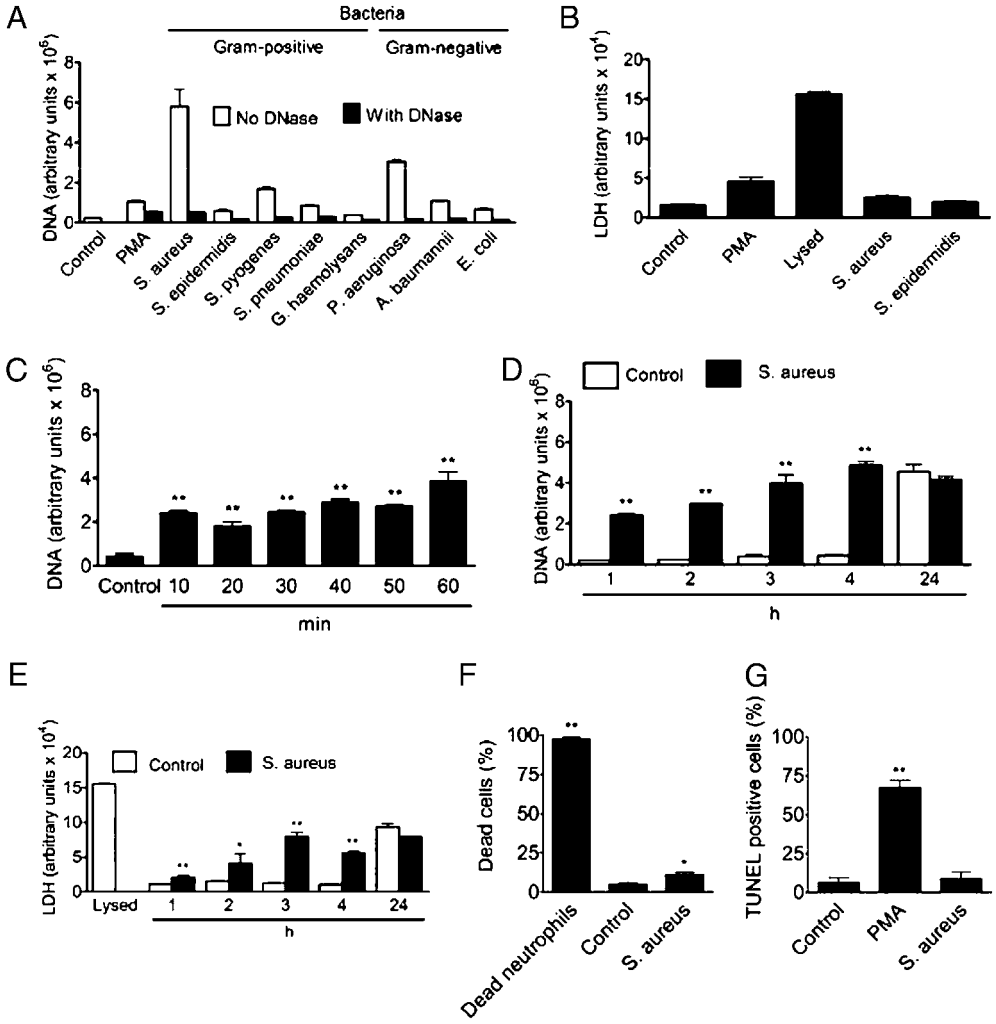

FIGURE 1. Human neutrophils release different amounts of neutrophil extracellular traps (NETs) depending on the bacterium due to a mechanism distinct from necrosis and apoptosis. *A*, Neutrophils were prepared from human donors. Bacteria were incubated to stationary phase, centrifuged, and suspended in normal saline. The number of bacteria included in samples was quantified according to nucleic acid staining results (24). Neutrophils and bacteria were incubated at a bacteria to neutrophil ratio of 10:1 for 1 h, and NETs were quantified with Sytox Green in a fluorescence microplate reader. Control: neutrophils alone. *B*, Neutrophils and bacteria were prepared as above, and LDH release was assessed with an enzymatic fluorometric assay. *C–E*, Neutrophils and *S. aureus* were incubated for (*C*) 10–60 min and (*D*) 1–24 h, and NETs were quantified and (*E*) LDH release measured. The data in *A–E* are presented as mean ± SD of triplicate samples and are representative of at least three experiments. $*p < 0.05$; $**p < 0.005$ versus control group. *F* and *G*, Neutrophils and *S. aureus* were prepared as before, incubated for 1 h, and studied with the (*F*) Live/Dead fixable dead cell stain kit and (*G*) APO-BrdU TUNEL assay kit and flow cytometry. The data in *F* and *G* are presented as mean ± SEM of at least three experiments. $*p < 0.05$; $**p < 0.005$ versus control group.

S. aureus to neutrophils. These conditions were used for the remainder of the experiments. NETs were detected within 10 min of *S. aureus* exposure increasing more subtly (2-fold) over the remaining 1 h (Fig. 1*C*) and doubling again by 4 h (Fig. 1*D*).

By 24 h, the DNA release was no longer due to *S. aureus* as neutrophils alone (Fig. 1*D*) or with PMA (data not shown) induced similar extracellular DNA levels presumably because all the cells were dead and lysed. Indeed, lysis of neutrophils was not a major part of *S. aureus*-induced NET induction until 2–3 h (Fig. 1*E*), an observation entirely consistent with Fuchs and colleagues (10) who described neutrophil lysis as a component of neutrophil NET formation beginning at 2 h and reaching peak levels at 3 and 4 h. Neutrophil viability assessed by flow cytometry was above 90% with and without *S. aureus* in the first hour (Fig. 1*F*). Heat-killed neutrophils all stained positive with a dead cell stain (97.2 ± 1.8%, mean ± SEM). Flow cytometry also revealed very few apoptotic neutrophils with or without *S. aureus,* whereas PMA at concentrations known to cause apoptosis caused more than 60% of neutrophils to be positive for APO-BrdU TUNEL (Fig. 1*G*). Clearly, during the first hour of NET formation with *S. aureus,* the neutrophils remained alive and not necrotic or apoptotic.

Recent studies suggested that mitochondrial DNA could be released from both eosinophils (11) and neutrophils (12). We prepared neutrophils and *S. aureus* as described previously, and NETs were studied with real-time PCR. Copies of both mitochondrial and nuclear genes were detected; however, nuclear DNA was in molar excess, with the vast majority of NET DNA (>100,000 times more) being of genomic rather than mitochondrial origin (data not shown).

Neutrophils respond to S. aureus *by releasing NETs, but not lysing*

Three complementary microscopy techniques were used to detect NET production. Neutrophils and bacteria or PMA were incubated only for 5 min and stained with Sytox Green. Immunofluorescence microscopy was used to detect early NET formation or neutrophil

uptake of Sytox Green (breach in membrane integrity). Very rarely was a neutrophil fluorescent in absence of any stimulus (Fig. 2*A*), but Sytox Green could be seen inside the neutrophils with high concentrations of PMA (marked with arrows) (Fig. 2*B*). By contrast, diffuse NET structures formed as early as 5 min after incubation with *S. aureus*, with no intracellular Sytox Green detected in any of the nearby cells (Fig. 2*C*). These fluorescent structures were completely abrogated if DNase was added at the end of incubation (Fig. 2*D*). With time, NETs filled the entire field of view (Fig. 2*E*). The surface area covered by NETs produced by *S. aureus* even after just 5-min incubation was much greater than that after stimulation with PMA (Fig. 2*F*).

Approximately 10–15% of neutrophils could be seen releasing NETs in response to *S. aureus* at 10 min (Supplemental Fig. 3). It is likely that some neutrophils had already released their NETs or numerous neutrophils released a small amount of DNA that was not detectable by microscopy, as 25% of total DNA was released at this early time point (Supplemental Fig. 4), according to the fluorescence DNA assay.

Scanning electron microscopy of untreated neutrophils revealed no NET production (Fig. 3*A*). With PMA, the neutrophils spread on the coverslips, but extracellular structures were not seen (Fig. 3*B*). Early NET release from otherwise intact neutrophils was seen in response to *S. aureus* (Fig. 3*C*). *S. aureus* was frequently covered by NETs (Fig. 3*D*), and the NET components appeared to form lattice-like structures (Fig. 3*E*). NETs appeared to be released through a small area on the neutrophil surface, and NETs from multiple neutrophils fused (Fig. 3*F*). Overt signs of neutrophil lysis were not detected.

Transmission electron microscopy revealed dramatic morphological changes in nuclear structure (Fig. 4). Whereas untreated neutrophils had clear polymorphonuclear appearance with intact nuclear membranes (Fig. 4*A*), after stimulation with *S. aureus,* neutrophils first underwent a massive dilation between the inner and outer nuclear membranes referred to as blebbing (Fig. 4*B*; magnified image in Fig. 4*C*). Within this inner and outer nuclear membrane separation are strands of DNA with bound nucleosomes in a repeated array showing a "beads on a string" ultrastructural appearance. This appearance is characteristic for strands of DNA with bound nucleosomes (Fig. 4*C*, strands shown by arrowhead; image magnified in Fig. 4*D*) reported in classical cell biology literature (27–30). The nucleosome "beads" measure an average of ~11 nm under high power (Fig. 4*D* arrowheads), which is consistent with reported literature of the diameter of nucleosomes wound by DNA. Some cells with dilatation of the nuclear envelope are surrounded by extracellular DNA NETs despite having intact plasma membranes (Fig. 4*E*). According to the published literature, the extracellular DNA NETs contain proteinaceous material, with granule contents, and an underlying DNA backbone with an average diameter of 50 nm (10), consistent with the NET shown in Fig 4*E*.

In later time points, there are vesicles seen in the cytoplasm of cells surrounded by DNA NETs (Fig. 5*A*, small arrowhead; image magnified in Fig 5*B*). Strikingly, within the lumen of the vesicles there are also "beads on a string" strands of DNA (Fig. 5*C*, arrowhead). It is worth noting that in the early stages of vesicle formation, the nuclei maintain intact nuclear pore complexes (Fig. 5*C*, star), and breakdown of the nuclear membrane

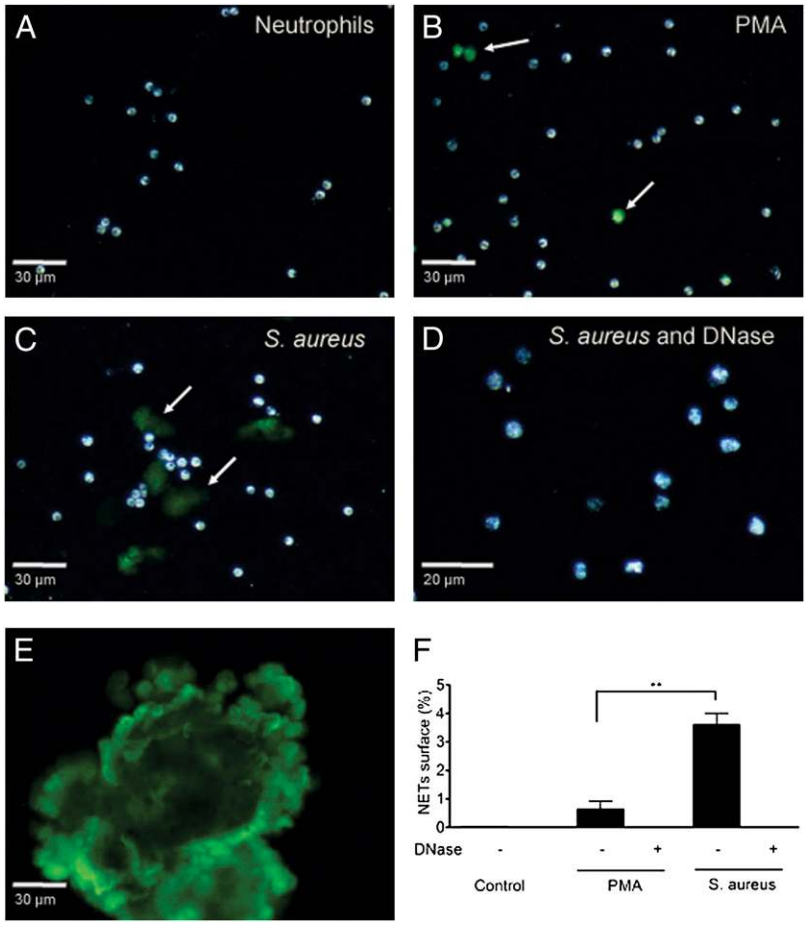

FIGURE 2. Microscopy images and quantification of NETs induced by *S. aureus*. Neutrophils and *S. aureus* were prepared as before and incubated for 5 min. Samples were stained with Sytox Green and studied on autologous plasma-coated glass slides with a fluorescent Richardson microscope and ×20 objective (*D* with ×40 objective). *A–D*, The images show neutrophils incubated alone (*A*), neutrophils incubated with PMA with arrows pointing to intracellular Sytox Green (*B*), neutrophils incubated with *S. aureus* and two of five NETs marked with arrows (*C*), and neutrophils incubated with *S. aureus* and DNase (*D*). The images of *A–D* were acquired with bright field light. *E*, Neutrophils were incubated with *S. aureus*, stained with Sytox Green, and the immunofluorescence image shows a conglomerate of NETs at a later time. The images (*A–E*) are representative of at least three experiments with neutrophils from different donors. Original magnification ×20. *F*, The surface area covered by the NETs was quantified per 100 neutrophils with image analysis software. The data are presented as mean ± SEM of three experiments. $^{**}p < 0.005$.

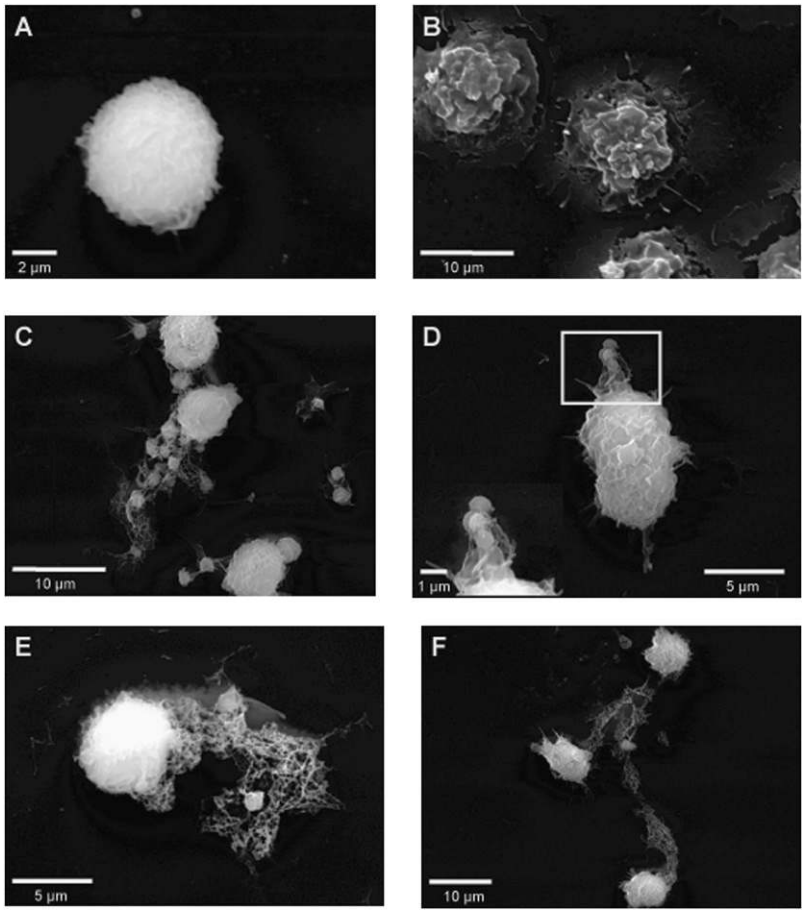

FIGURE 3. Scanning electron microscopy of NETs after incubation with *S. aureus*. Neutrophils and *S. aureus* were incubated for 1 h on autologous plasma-coated slides, fixed with glutaraldehyde, stained with a gold film (see *Materials and Methods*), and studied with scanning electron microscopy. *A*, Neutrophils alone. *B*, Neutrophils stimulated with PMA. *C–F*, Neutrophils incubated with *S. aureus*: (*D*) *S. aureus* was covered by NETs; (*E*) NETs formed lattice-like structures and entangled *S. aureus*; (*F*) NETs were seen emanating from a small area on the neutrophil surface and fused to other NETs. The images are representative of three experiments with neutrophils from different donors.

was not evident despite DNA clearly outside the cell (Fig 4*E* and Fig. 5*A*). As many vesicles continue to bud from the nuclear envelope, the nuclei become rounded with uniformly condensed chromatin (Fig. 5*D*). These nuclei also contain the large nuclear envelope dilatations (Fig. 5*D*, arrowhead). A DNA-containing vesicle is seen budding off the nuclear envelope (Fig. 5*F*, arrowhead), and many vesicles can be seen as separate entities in the cytoplasm (Fig. 5*E*, 5*F*). During this stage, cytoplasmic dense granules are also seen lining up along the intact plasma membrane (Fig. 5*F*).

Neutrophils eventually undergo completion of nuclear envelope breakdown, releasing DNA material into the cytoplasm with tubules of nuclear envelope (Fig. 6*A*, 6*B*, small arrowheads) detaching from underlying chromatin (Fig. 6*A*, 6*B*, large arrowheads). The ultrastructure of these events is virtually identical to nuclear envelope breakdown in prometaphase in mammalian cells (31). The vesicles released from the nuclear envelope are seen at the plasma membrane (Fig. 6*C*). The vesicles containing DNA strands are released into the extracellular space (Fig. 6*D*, small arrowhead) where they then lyse and empty their contents to form NETs (Fig. 6*E*, large arrowhead). Some dense cytoplasmic granules are also released into the extracellular space (Fig. 6*C*, arrowhead), whereas others are seen fusing with the plasma membrane to empty their contents (Fig. 6*E*, small arrowhead), consistent with published reports of NETs containing granule contents. These images suggest the contents of granules and DNA vesicles mix in the extracellular space. Some anuclear cells contain DNA material throughout the cytoplasm while entangling bacterial clusters in a DNA NET (Fig. 6*F*, arrowhead).

To elucidate the timing of these events, a total of 50 randomly selected cells at each time point ($n = 200$) were quantified in the em for the different obvious morphologies over time (experiment repeated to measure intraobserver error). As time progressed from 5 min to 1 h, after neutrophil incubation with *S. aureus*, there was a linear decrease of cells with intact nuclei and an inverse increase in cells undergoing nuclear envelope dilation, nuclear condensation, and nuclear envelope breakdown (Fig. 6*G*). Nuclear dilatations were seen most frequently at early time points (25 min), whereas nuclear condensation peaked at 45 min, and complete nuclear envelope breakdown was most frequently seen at 60 min. This suggests that a neutrophil likely undergoes morphological changes in a specific order: 1) nuclear envelope dilation and vesicular formation and release, 2) nuclear condensation, followed by 3) nuclear envelope breakdown. Lytic release of DNA from neutrophils was not seen in the first 60 min. The entire population of neutrophils in an incubation doing this in an asynchronous manner with DNA being extruded into NETs via a mechanism is consistent with the biochemical and fluorescent imaging data where NET formation from a neutrophil occurs in less than 20 min.

NETs are caused primarily by released bacterial products

It is possible that molecules released from *S. aureus* contribute to NET production. Indeed, supernatant concentrates from *S. aureus* grown to stationary phase for 12 h and filter-sterilized induced ample NETs but had to be diluted due to increased concentrations of all proteins over this growth period (Fig. 7*A*). Low dilutions (1/24) of supernatant incubated with neutrophils caused a large amount of DNA release but LDH increased to the same level as was observed with lysed cells (Fig. 7*A*) indicating complete neutrophil lysis. Samples with dilutions of 1/493 and 1/2466 induced similar levels of NET production as live bacteria with no significant increase in LDH (Fig. 7*A*). To ensure that it was not the 12-h incubation that was necessary for the NET production via

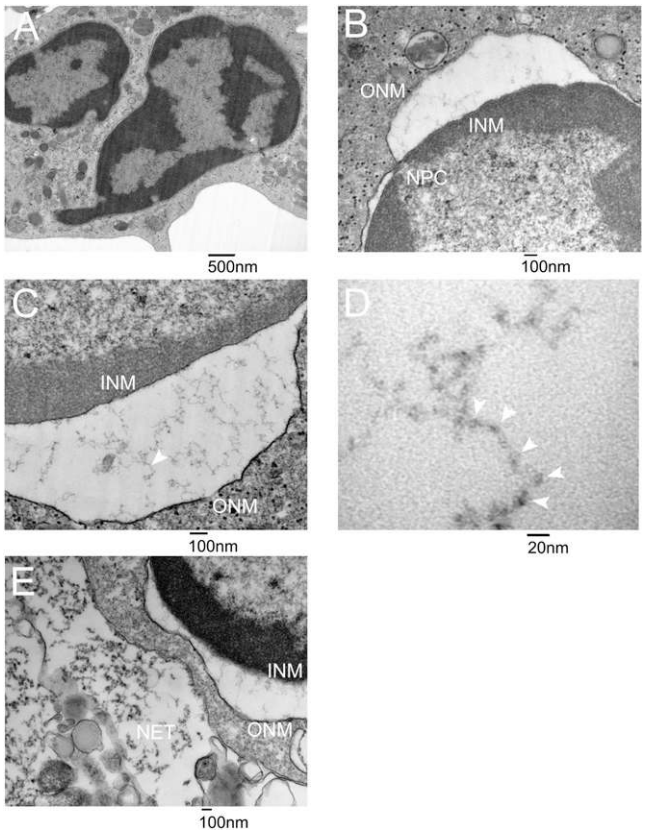

FIGURE 4. Transmission electron microscopy of NET formation showing nuclear envelope alterations. Neutrophils and *S. aureus* were prepared as before, and after fixation with glutaraldehyde they were processed and studied with transmission electron microscopy. Images were obtained from samples with neutrophils alone (*A*) and neutrophils incubated with *S. aureus* (*B–E*). *B* and *C* show neutrophils displaying separation of inner nuclear membrane (INM) from outer nuclear membrane (ONM). The nuclear pore complex (NPC) is shown as a marker of INM and ONM. There are small DNA strands with characteristic, previously published "beads on a string" appearance within the lumen between the INM and ONM measuring an average of 11 nm in diameter (strand in *C*, arrowhead, is magnified in *D*, arrowheads display the repeated array or "beads on a string"). Cells with nuclear dilations at early time points are surrounded by NETs (*E*). Original magnifications ×10,000 (*A*), ×20,000 (*B*), ×30,000 (*C*), ×80,000 (*D*), ×20,000 (*E*), and ×10,000 (*F*) using 60 kV voltage. Sections were stained with uranyl acetate and lead citrate (see *Materials and Methods*). Scale bars are as shown.

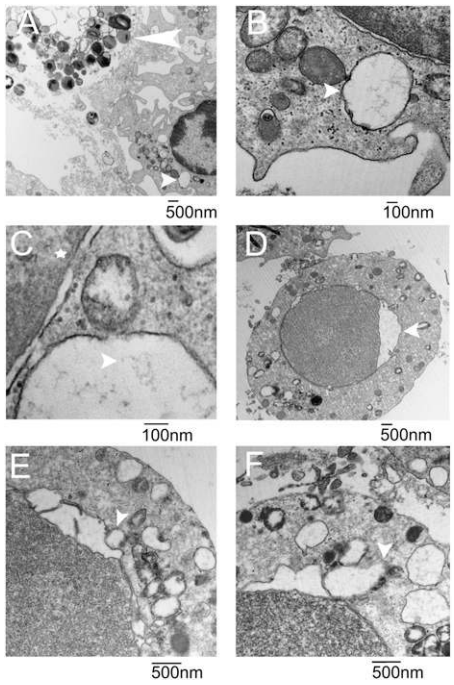

FIGURE 5. Transmission electron microscopy of NET formation showing nuclear vesicle formation. *A–F*, Images were obtained from samples with neutrophils incubated with *S. aureus*. Images show neutrophils with DNA containing vesicles in the cytoplasm (*A*, small arrowhead) with extracellular NETs containing bacteria (*A*, large arrowhead). Enlarged view of vesicle (*B*, arrowhead) containing DNA strands (*C*, arrowhead). These nuclei have intact nuclear pore complexes present (*C*, star). Neutrophils with rounded condensed nuclei and intact nuclear envelope are seen in later stages of NET formation (*D*). These nuclei also contain nuclear envelope dilatations (arrowhead) and DNA vesicles in the cytoplasm (*D*). Vesicles are seen budding off the nuclear envelope (*E* and *F*, arrowhead) with cytoplasmic granules migrating to the plasma membrane. Original magnifications ×3,000 (*A*), ×20,000 (*B*), ×30,000 (*C*), ×3,000 (*D*), ×10,000 (*E*), and ×10,000 (*F*) using 60 kV voltage. Sections were stained with uranyl acetate and lead citrate (see *Materials and Methods*). Scale bars are as shown.

supernatant, supernatants from bacteria incubated for brief periods (30 min) or the use of semipermeable membranes to separate neutrophils from bacteria demonstrated that there was physiologic ongoing release of mediators from *S. aureus* that induced NET production (data not shown). This activity could be abolished by addition of proteinase K suggesting a protein(s) is responsible for the NETs (Fig. 7*A*).

Using ion-exchange and size-exclusion chromatography, samples were fractionated, and active fractions were identified using our standard NET fluorescence assay (Supplemental Fig. 5). The active fractions were subjected to mass spectrometry, and three proteins were the most frequently found proteins in the fractions with activity. These included PVL and more specifically the LukS (component), autolysin (*N*-acetylmuramyl-L-alanine amidase and *endo*-b-*N*-acetylglucosaminidase), and a lipase (glycerol ester hydrolase).

Next, recombinant autolysin was used to determine whether this protein could induce NET formation (Fig. 7*B*). There was no increase in NET formation when a concentration of 0.125 μg/m autolysin was used. Increasing the autolysin concentrations to above 1 μg/ml doubled the amount of NET release, and further increasing the concentration 5-fold did not further increase NET production. This makes autolysin a very minor NET inducer. Less than 5% of neutrophils incubated with recombinant autolysin produced NETs. No increase in LDH or propidium iodide was detected (data not shown).

PVL has two components, LukF and LukS. LukF alone (up to 6.0 μg/ml) and LukS alone (up to 54 μg/ml) induced NET formation (data not shown). However, as little as 0.2 μg/ml of the two components together (Fig. 7*C*) induced some NET release, and at 0.7 μg/ml, 50% of total DNA was released (relative to lysed cells) with no detectable LDH release (data not shown). Higher concentrations of PVL (~3 μg/ml) significantly increased the amount of LDH release, so these concentrations were not studied further. Propidium iodide staining to detect dead cells confirmed very low numbers of dead cells with 0.7 μg/ml PVL or lower (data not shown). DNase abolished the fluorescence suggesting the fluorescence was a result of DNA (data not shown).

Antiserum against PVL but not against autolysin decreased NET formation caused by S. aureus *supernatant*

The third major component identified in *S. aureus* supernatant was lipase. Although no recombinant or isolated lipase was available, a strain of *S. aureus* (MW2 geh::psk950) that does not produce

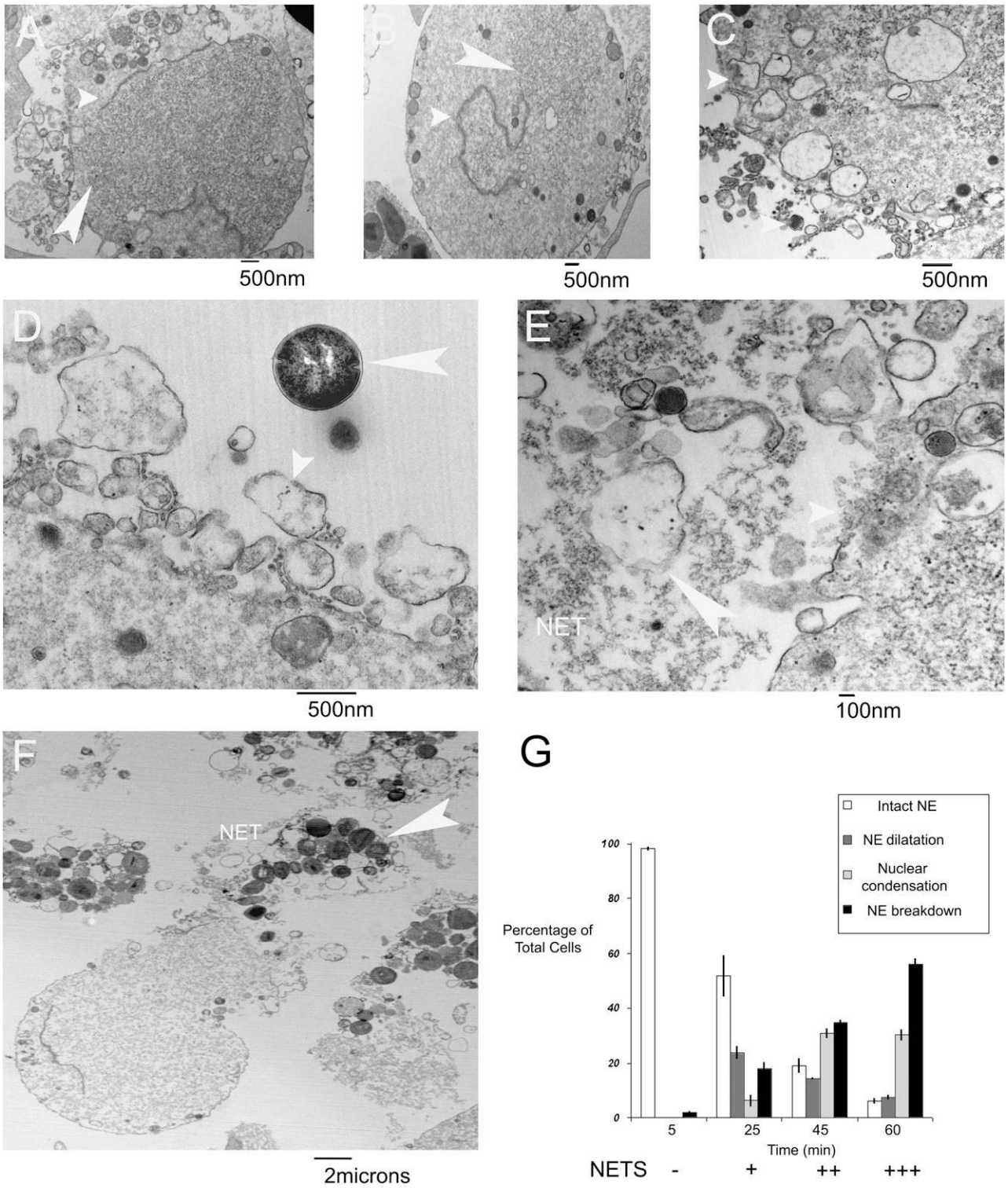

FIGURE 6. Transmission electron microscopy of NET formation showing end stages of nuclear breakdown. Neutrophils and *S. aureus* were prepared as before and studied with transmission electron microscopy. *A–F*, Images were obtained from samples with neutrophils incubated with *S. aureus*. In *A* and *B*, neutrophils undergoing completion of nuclear envelope breakdown are shown containing tubules of nuclear envelope (small arrowheads) detaching from underlying chromatin (large arrowheads). Vesicles containing DNA strands are seen fusing with the outer plasma membrane (*C*, *upper small arrowhead*) and some released directly into the extracellular space (*C–E*, containing DNA strands shown by the arrowhead) in response to bacteria (*D*, large arrowhead). The vesicles are seen lysing and releasing their content in the extracellular space to form NETs (*E*, large arrowhead). Granules are seen in the extracellular space (*C, small lower arrowhead*) and also fusing with the plasma membrane (*E*, small arrowhead). An anuclear cell is shown that has undergone completion of nuclear envelope breakdown (*F*). DNA material was released through the plasma membrane and has formed bacterial clusters within NETs (*F*, arrowhead). A total of 50 randomly selected cells at each time point were quantified for different morphological changes (experiment repeated to measure intraobserver SE, $n = 200$ for each experiment) (*G*). There were statistically significant changes in nuclear morphologies over the 1-h experiment with a linear increase in cells undergoing nuclear envelope breakdown (ANOVA, p value <0.01, SE bars included). Original magnifications ×5,000 (*A*), ×5,000 (*B*), ×8,000 (*C*), ×12,000 (*D*), ×15,000 (*E*), and ×2,000 (*F*) using 60 kV voltage. Sections were stained with uranyl acetate and lead citrate (see *Materials and Methods*). Scale bars are as shown.

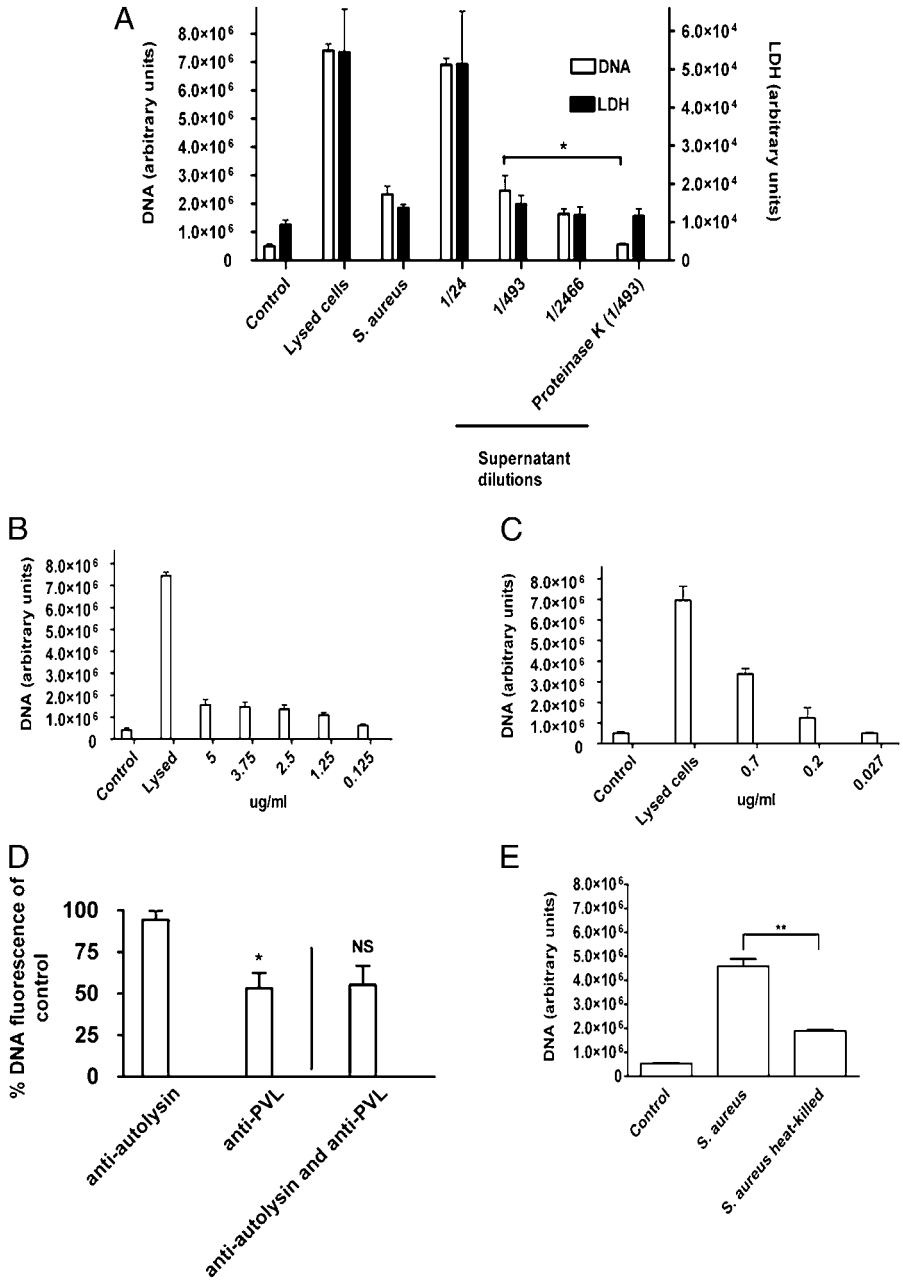

FIGURE 7. NETs are caused by surface factors and products released by bacteria. *S. aureus* supernatants from 12-h stationary-phase cultures were filter-sterilized, diluted 1/24, 1/493, and 1/2466, and studied with neutrophils as before. Both DNA (left axis and empty bars) and LDH (right axis and filled bars) are presented. *A*, Proteinase K inhibited DNA release at 1/493 dilution without increasing LDH. $*p < 0.05$. *B* and *C*, Very subtle increases in DNA release with autolysin (*B*) with much greater DNA release with PVL (*C*) were noted. *D*, Antiserum against PVL, autolysin, or both was incubated with supernatant without lipase, and inhibition of NET production was examined. Percentage inhibition is shown. $*p < 0.05$. The data (*A–D*) are presented as mean ± SEM of three experiments. *E*, *S. aureus* was killed by exposure to 80°C for 20 min and subsequently used in the NET quantification assay (*E*). The data (*E*) are presented as mean ± SD of triplicate samples and are representative of three experiments. $**p < 0.005$.

lipase still produced ample NETs excluding this molecule as a potential NET-inducing molecule (data not shown).

In the next experiment, antisera against autolysin and/or PVL were used. Whereas autolysin antiserum did not inhibit NET production, antiserum against PVL inhibited NET production by ~50%, and this value was not further improved by either the addition of autolysin antiserum or testing the role of PVL in lipase-deficient supernatant with or without autolysin antiserum (Fig. 7*D*). Inhibition of NET formation with antiserum against PVL and autolysin was not different between supernatants of lipase-deficient *S. aureus* and parent strain.

Neutrophils responded to metabolically inactive *S. aureus* (dead bacteria) with NET production, but the response was much smaller than that with live *S. aureus* (Fig. 7*E*), suggesting an important role for the soluble bacterial metabolites and mediators.

NET formation caused by different S. aureus *strains*

S. aureus ATCC 25923 strain was used for the majority of this study. We also tested *S. aureus* strains including USA 400, which produces PVL and can cause serious infections in humans. This strain is also known as community-acquired methicillin-resistant *S. aureus*. By contrast, M92 is a strain of *S. aureus* that was grown from a healthy person as a colonizing strain. *S. epidermidis*, tested as a negative control *Staphylococcus* species, often grows on human skin without causing disease and causes less rapid and frequent tissue destruction during infection. No difference in the quantity of NETs formed was seen between ATCC 25923 and USA 400, but more NETs were formed by ATCC 25923 compared with the colonizer M92 and *S. epidermidis* (data not shown). In summary, the amount of NET formation differs between different strains and may correlate with degree of pathogenesis.

Early formation of NETs by S. aureus *is independent of ROS produced by NADPH oxidase*

When oxidant production by neutrophils was examined, PMA induced oxidant production within 2 min. By contrast, *S. aureus* did not produce detectable levels of oxidants at 10 min despite ample NET production (Supplemental Fig. 6). By 30 min. *S.*

aureus was causing significant oxidant production (Supplemental Fig. 6). This delay may be due to time to phagocytosis or due to the antioxidant properties of *S. aureus*. Inhibition of NADPH oxidase with DPI was previously shown to abolish NET production effectively when neutrophils were stimulated for 4 h (10). No inhibition of NET production was detected when DPI was administered and then neutrophils were co-incubated with *S. aureus* at any time point over the first hour (Fig. 8*A* and Supplemental Fig. 6). DPI at this concentration prevented PMA-stimulated neutrophil oxidant production as effectively as the free radical scavenger superoxide dismutase (Fig. 8*B*). DPI could inhibit NET production over longer incubation periods with *S. aureus*; 30% at 2 h and by 80% at 3 and 4 h (Fig. 8*C*). The fact that the oxidant-independent NETs formed at 1 and 2 h but were no longer present at 3 h suggests that there was a continuous degradation of NETs, an observation consistent with the fact that *S. aureus* releases DNases that help the bacterium degrade and escape NETs (15).

Early NETs can kill S. aureus *but have limited proteolytic activity*

Neutrophils were co-incubated with *S. aureus* and DNase for 1 h (0 min), and then samples were obtained for overnight growth and CFU determination (Fig. 8*D*). The results demonstrate a very significant ability of neutrophils to kill *S. aureus* that was impaired when NET formation was limited with DNAse: *S. aureus* viability was increased significantly (Fig. 8*D*). However, neutrophils co-incubated with varying concentrations of *S. aureus* with DNase added during the last 5 min of incubation did reveal some increased survival (Supplemental Fig. 7). Indeed at low concentrations of *S. aureus,* as much as 10-fold greater amounts of free bacteria were detected in the presence of DNase, suggesting that live bacteria trapped in NETs can be released after dissolving NETs with DNase at low concentrations of *S. aureus*.

Previous reports have demonstrated that NETs have elastase immobilized to their surface. Elastase activity associated with the NETs as a measure of proteolytic activity was not detected in the first 10 min (data not shown) but was detected in response to *S. aureus* within the first hour. However, it was substantially less than the amount measured at 4 h when lysis was the dominant mechanism of NET production (Fig. 8*E*). Clearly, the NETs can kill bacteria very effectively, but the neutrophils do not release all their granular content. In addition to elastase as a hallmark feature of NETs, we were also able to see histones associated with the early NET production, and this molecule also has ample bactericidal activity (32).

Finally, to ensure that these experiments were not an in vitro artifact, we also examined NET production in vivo by s.c. injection of *S. aureus* and subsequent examination of neutrophil behavior using spinning disk microscopy as previously described (33). We clearly observed an increase in NET production from neutrophils within 10 min of *S. aureus* exposure. Moreover, the NETs were associated with histones (data not shown).

Discussion

The fact that *S. aureus* can cause systemic and severe localized infection in otherwise healthy children and adults underscores the importance of understanding how this pathogen manages to evade

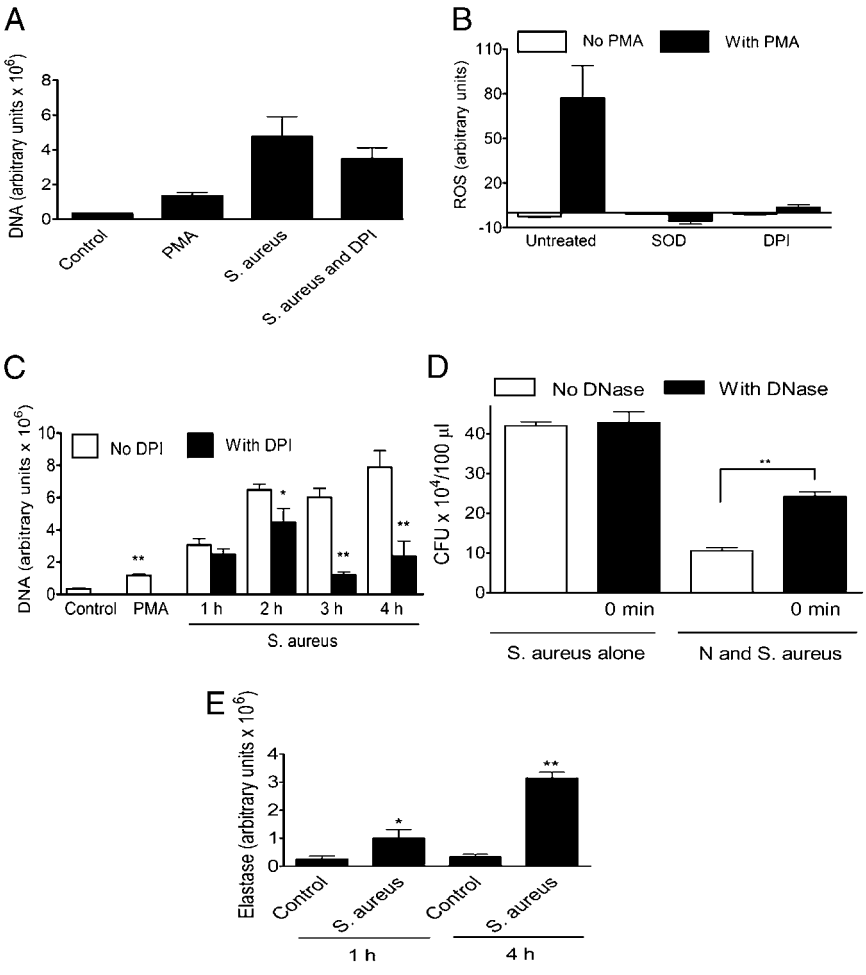

FIGURE 8. NETs are formed during inhibition of NADPH oxidase and can kill *S. aureus* but have limited proteolytic activity. *A*, Neutrophils and *S. aureus* were prepared as before, and NADPH oxidase was inhibited with DPI. NETs were quantified with Sytox Green in a fluorescence microplate reader. The data are presented as mean ± SEM from seven experiments. *B*, Neutrophils were purified and cytochrome c was added. To quantify ROS, cytochrome c reduction was detected with a spectrophotometer. Samples were also incubated with DPI or superoxide dismutase (SOD) before stimulation with PMA as indicated. The data are presented as mean ± SEM from four experiments. *C*, Neutrophils and bacteria were prepared as before with or without DPI and incubated for the indicated times. NETs were quantified with Sytox Green. The data are presented as mean ± SD of triplicate samples and are representative of three experiments. $*p < 0.05$; $**p < 0.005$ versus control group. *D*, Neutrophils and *S. aureus* were incubated with DNase for 1 h (0 min), and subsequently samples were obtained and grown overnight on culture plates for CFU counting. The data are presented as mean ± SEM from three experiments. $**p < 0.005$ versus control group. *E*, Neutrophils and *S. aureus* were prepared as before, and neutrophil elastase was quantified with EnzChek elastase assay kit at 1 or 4 h. The data are presented as mean ± SEM from three experiments. $*p < 0.05$ or $**p < 0.005$ versus control group.

the host innate immune system. In this regard, *S. aureus* has evolved multiple ways of inhibiting immune defense mechanisms. *S. aureus* disrupts complement activation by secreting *Staphylococcus* complement inhibitor (16) and expressing clumping factor on the cell wall (17) thereby preventing opsonization. Moreover, *S. aureus* can interfere with neutrophil receptors that bind Ab bound to the bacteria (18). Moreover, *S. aureus* also has evolved inhibitory mechanisms of oxidant production by neutrophils. Indeed, the golden pigment for which *S. aureus* is named is a potent antioxidant (34), and *S. aureus* produces abundant amounts of superoxide dismutase and catalase such that marginal oxidative burst function is detected from neutrophils infected with this pathogen (35, 36). This is very important because as previously mentioned, oxidants are critical for NET production via cell lysis, raising the possibility that neutrophils will be incapable of producing NETs. *S. aureus* also secretes numerous molecules that can lyse neutrophils so a rapid, extracellular killing mechanism that functions independent of oxidant production might be optimal for *S. aureus* killing. Indeed, this study has identified a novel process of NET release in response to *S. aureus* that is radically different from the lytic pathway described by Fuchs and colleagues (10).

Other Gram-positive or Gram-negative bacteria induced NETs to a much lesser magnitude at these early time points. Incubation with *S. aureus* for 10 min was sufficient for substantial NET formation, despite minimal neutrophil lysis, death, or apoptosis. This suggests a coordinated mechanism of chromatin release as a rapid defense mechanism against invading bacteria. Indeed, a very striking transformation of the nucleus occurred over the first few minutes that included a very rapid morphological change from polymorphonuclear to a condensed sphere. This included a separation of the inner and outer nuclear envelope and budding of vesicles, where both separated envelopes and vesicles were filled with nuclear DNA. Then the DNA was released from a discrete site on the plasma membrane into the extracellular space. Notably, the DNA-containing vesicles could be seen in the extracellular space suggesting the release of intact vesicles rather than nuclear and plasma membrane fusion. The released DNA was primarily of nuclear not mitochondrial origin.

Unlike the original demonstration of NET production (10), the very rapid NET formation described in the current study occurred independent of oxidants. In fact, 10-min exposure of neutrophils to *S. aureus* was not sufficient time to detect oxidants (Supplemental Fig. 6), yet NETs were already forming in that time frame (Fig. 1*C*). In fact, *S. aureus* has numerous antioxidant mechanisms likely explaining the limited or delayed production of oxidants relative to a compound like PMA. It is our contention that the early NET production is dependent on vesicular exocytosis, and the nuclear envelope disintegration likely leads to filling of the cytoplasm with DNA and the ultimate lysis of the cell releasing all intracellular contents including the classical NETs that were originally described (1, 10). It is however conceivable that some of the nonlytic NET production does involve nuclear envelope breakdown, which can occur via numerous other oxidant-independent mechanisms. Indeed, during cell division the nuclear envelope disintegrates independent of oxidants (37) and is dependent on microtubule-associated motor protein dynein (31). Further evidence that oxidants were unlikely to be the underlying mechanism in rapid NET production is that PMA within minutes causes robust, near-maximal oxidant production from neutrophils, and yet at least 3 h is required for NET production to occur under these circumstances (10).

NET-inducing factors identified to date include IL-8, PMA, bacteria, mycobacteria, fungi (38), protozoa (4), platelet-activating factor, LPS (39), and M1 protein (40). The components of NET structures may be influenced by the stimulant, because after stimulation with C5a, NETs contained mitochondrial DNA (12). The *S. aureus* supernatant used in this study contained a number of potential NET-inducing factors. *S. aureus* releases numerous factors that could cause NETs, but PVL is worth mentioning. PVL is a pore-forming toxin and depending on the concentration causes cell death by necrosis or by apoptosis (41). Neutrophils exposed to *S. aureus* in our study were not apoptotic, necrotic, or overtly ruptured, arguing against high, lysing concentrations of PVL as the NET-inducing agent. However, it is possible that lower concentrations of PVL induce NETs, whereas higher concentrations induce lysis. Our experiments revealed a concentration of PVL that did indeed induce NETs without cell lysis. However, our data suggest that there are other as yet unidentified molecules aside from PVL that contribute to NET formation. Our data also suggest that not all pore-forming molecules necessarily induce NETs as autolysin had only minor NET-inducing properties, and *S. pneumoniae*, which produces cholesterol-dependent cytolysin pneumolysin, did not induce large amounts of NETs. *S. pyogenes*, which releases the β-pore-forming toxin hemolysin, did induce moderate levels of NETs. Therefore, the possibility that PVL and some other molecules cause NET production inducing severe collateral tissue damage during human infections is intriguing and potentially of great therapeutic interest (14).

The different imaging approaches presented in this study show the cell nucleus changing from polymorphonuclear to spherical and then NETs emerging in a localized area on the neutrophil surface. Based on the transmission electron microscopy, initial NET formation could be via vesicular release. This could indicate a regulated extrusion of chromatin at the neutrophil surface. However, we also saw anuclear neutrophils with DNA throughout the cytoplasm suggesting also a nonvesicular mechanism of NET formation, which may be related to the more "classical" lytic NET production described by Fuchs and colleagues (10). This process is unlikely to be similar to RBC expulsion of the intact cell nucleus, followed by resealing of the erythrocyte cell surface (42). Although neutrophils can also reseal after the removal of nuclei through vigorous centrifugation (13), our data do not support the release of the entire nucleus all at once. However, it is worth noting that loss of the nucleus in neutrophils does not spell the end of that cell. Indeed, the latter study (13) reported that removal of nuclei from neutrophils would not prevent chemotaxis, adherence, phagocytosis, or bacterial killing. In fact, in preliminary experiments, we observed neutrophils releasing their DNA in response to *S. aureus* in tissues and then continue to crawl in the tissues (B.G. Yipp and P. Kubes, unpublished observations).

This raises intriguing questions about the mechanism involved in the formation of NETs. The transmission electron microscopy images displayed a dramatic separation of the inner and outer nuclear membranes containing chromatin. These deformations of the nuclear envelope are strikingly similar to the ultrastructure from mouse embryo fibroblasts homozygous for the lamin A deletion (43). In fact, numerous heritable human diseases called "laminopathies" exist that display clinical phenotypes from nuclear lysis due to fragility of the nuclear envelope. More interestingly, studies from patients with a defective nuclear envelope protein called emerin show evidence of similar dilatations and deformations of the nuclear envelope whereby heterochromatin is lost into the elements of the endoplasmic reticulum (43). The changes described in patients (43) are very similar to the changes observed in this study, where neutrophils activated by bacteria displayed bizarre nuclear morphologies with chromatin material found within the dramatically dilated lumen of the nuclear envelope, endoplasmic reticulum, and within vesicles released into the cytoplasm.

The linker of nucleoskeleton and cytoskeleton complex represents the cell protein connections between the nuclear envelope and cytoskeletal elements (44–46). Neutrophils have been previously found to be missing numerous proteins of the linker of nucleoskeleton and cytoskeleton protein complex, which spans both the inner and outer nuclear membranes and is attached to the outer actin cytoskeleton (44). Whether this natural defect is present to permit NET formation remains unknown. It is intriguing that the process of NET formation is associated with nuclear envelope breakdown ultrastructurally similar to mitotic cells with sheets of nuclear membrane detaching from chromatin (31). The latter mechanism is facilitated by microtubule motor proteins, and in fact inhibition of tubulin polymerization and actin filamentation decrease formation of NET structures (47). Further studies are required to elucidate the nuclear changes of NET formation, for example, the role of nuclear envelope proteins and the outer cytoskeleton, and possible exocytosis of DNA-containing vesicles arising from disrupted chromatin or inner nuclear membrane protein interactions.

Our data suggest that the rapid NET formation described in this study has the capacity to ensnare and kill bacteria and perhaps prevent their dissemination. We propose that the rapid release of NETs may be essential to wall off the infection (e.g., during infections of the skin with abscess formation). This would allow the neutrophil to phagocytose NET-immobilized bacteria and/or kill them with oxidants, proteases, and perhaps even via more toxic NETs released at later time points. It is intriguing that in chronic infections in cystic fibrosis patients, DNAse is used as an inhalant to help liberate mucous plugs but will almost certainly affect NET formation in these chronically infected patients. The implication of disrupting NET formation in this condition remains to be elucidated. It should not be forgotten that NETs can harm surrounding tissue (3), and this particularly avid release of NETs with *S. aureus* could explain some of the notable tissue necrosis caused by this increasingly problematic pathogen.

Acknowledgments

We thank Derrice Knight, Gustavo Menezes, Hong Zhou, Lori Zbytnuik, Chris Waterhouse, Bjoern Petri, and Marlene Manson for help with editing of figures and the manuscript. We thank Dr. David Hooper (Massachusetts General Hospital, Boston, MA) for providing *S. aureus* (MW2 geh::psk950) and parent strain. We thank Elaine Yung for processing and cutting the EM samples and the Calgary Laboratory Services Imaging Facility. We thank the Microbial Communities Core Facility at the University of Calgary, as well as the Canadian Foundation for Innovation.

Disclosures

The authors have no financial conflicts of interest.

References

1. Brinkmann, V., U. Reichard, C. Goosmann, B. Fauler, Y. Uhlemann, D. S. Weiss, Y. Weinrauch, and A. Zychlinsky. 2004. Neutrophil extracellular traps kill bacteria. *Science* 303: 1532–1535.
2. Gupta, A. K., P. Hasler, W. Holzgreve, S. Gebhardt, and S. Hahn. 2005. Induction of neutrophil extracellular DNA lattices by placental microparticles and IL-8 and their presence in preeclampsia. *Hum. Immunol.* 66: 1146–1154.
3. Clark, S. R., A. C. Ma, S. A. Tavener, B. McDonald, Z. Goodarzi, M. M. Kelly, K. D. Patel, S. Chakrabarti, E. McAvoy, G. D. Sinclair, et al. 2007. Platelet TLR4 activates neutrophil extracellular traps to ensnare bacteria in septic blood. *Nat. Med.* 13: 463–469.
4. Guimarães-Costa, A. B., M. T. Nascimento, G. S. Froment, R. P. Soares, F. N. Morgado, F. Conceição-Silva, and E. M. Saraiva. 2009. *Leishmania* amazonensis promastigotes induce and are killed by neutrophil extracellular traps. *Proc. Natl. Acad. Sci. USA* 106: 6748–6753.
5. Kessenbrock, K., M. Krumbholz, U. Schönermarck, W. Back, W. L. Gross, Z. Werb, H. J. Gröne, V. Brinkmann, and D. E. Jenne. 2009. Netting neutrophils in autoimmune small-vessel vasculitis. *Nat. Med.* 15: 623–625.
6. Beiter, K., F. Wartha, B. Albiger, S. Normark, A. Zychlinsky, and B. Henriques-Normark. 2006. An endonuclease allows *S. pneumoniae* to escape from neutrophil extracellular traps. *Curr. Biol.* 16: 401–407.
7. Buchanan, J. T., A. J. Simpson, R. K. Aziz, G. Y. Liu, S. A. Kristian, M. Kotb, J. Feramisco, and V. Nizet. 2006. DNase expression allows the pathogen group A *Streptococcus* to escape killing in neutrophil extracellular traps. *Curr. Biol.* 16: 396–400.
8. Walker, M. J., A. Hollands, M. L. Sanderson-Smith, J. N. Cole, J. K. Kirk, A. Henningham, J. D. McArthur, K. Dinkla, R. K. Aziz, R. G. Kansal, et al. 2007. DNase Sda1 provides selection pressure for a switch to invasive group A streptococcal infection. *Nat. Med.* 13: 981–985.
9. Sumby, P., K. D. Barbian, D. J. Gardner, A. R. Whitney, D. M. Welty, R. D. Long, J. R. Bailey, M. J. Parnell, N. P. Hoe, G. G. Adams, et al. 2005. Extracellular deoxyribonuclease made by group A *Streptococcus* assists pathogenesis by enhancing evasion of the innate immune response. *Proc. Natl. Acad. Sci. USA* 102: 1679–1684.
10. Fuchs, T. A., U. Abed, C. Goosmann, R. Hurwitz, I. Schulze, V. Wahn, Y. Weinrauch, V. Brinkmann, and A. Zychlinsky. 2007. Novel cell death program leads to neutrophil extracellular traps. *J. Cell Biol.* 176: 231–241.
11. Yousefi, S., J. A. Gold, N. Andina, J. J. Lee, A. M. Kelly, E. Kozlowski, I. Schmid, A. Straumann, J. Reichenbach, G. J. Gleich, and H. U. Simon. 2008. Catapult-like release of mitochondrial DNA by eosinophils contributes to antibacterial defense. *Nat. Med.* 14: 949–953.
12. Yousefi, S., C. Mihalache, E. Kozlowski, I. Schmid, and H. U. Simon. 2009. Viable neutrophils release mitochondrial DNA to form neutrophil extracellular traps. *Cell Death Differ.* 16: 1438–1444.
13. Malawista, S. E., G. Van Blaricom, and M. G. Breitenstein. 1989. Cryopreservable neutrophil surrogates. Stored cytoplasts from human polymorphonuclear leukocytes retain chemotactic, phagocytic, and microbicidal function. *J. Clin. Invest.* 83: 728–732.
14. Gordon, R. J., and F. D. Lowy. 2008. Pathogenesis of methicillin-resistant *S. aureus* infection. *Clin. Infect. Dis.* 46(Suppl 5): S350–S359.
15. Nizet, V. 2007. Understanding how leading bacterial pathogens subvert innate immunity to reveal novel therapeutic targets. *J. Allergy Clin. Immunol.* 120: 13–22.
16. Rooijakkers, S. H., M. Ruyken, A. Roos, M. R. Daha, J. S. Presanis, R. B. Sim, W. J. van Wamel, K. P. van Kessel, and J. A. van Strijp. 2005. Immune evasion by a staphylococcal complement inhibitor that acts on C3 convertases. *Nat. Immunol.* 6: 920–927.
17. Higgins, J., A. Loughman, K. P. van Kessel, J. A. van Strijp, and T. J. Foster. 2006. Clumping factor A of *S. aureus* inhibits phagocytosis by human polymorphonuclear leucocytes. *FEMS Microbiol. Lett.* 258: 290–296.
18. Agniswamy, J., B. Lei, J. M. Musser, and P. D. Sun. 2004. Insight of host immune evasion mediated by two variants of group a *Streptococcus* Mac protein. *J. Biol. Chem.* 279: 52789–52796.
19. Gresham, H. D., J. H. Lowrance, T. E. Caver, B. S. Wilson, A. L. Cheung, and F. P. Lindberg. 2000. Survival of *S. aureus* inside neutrophils contributes to infection. *J. Immunol.* 164: 3713–3722.
20. Kim, W., and M. G. Surette. 2004. Metabolic differentiation in actively swarming *Salmonella. Mol. Microbiol.* 54: 702–714.
21. Ding, Y., Y. Onodera, J. C. Lee, and D. C. Hooper. 2008. NorB, an efflux pump in *S. aureus* strain MW2, contributes to bacterial fitness in abscesses. *J. Bacteriol.* 190: 7123–7129.
22. Labandeira-Rey, M., F. Couzon, S. Boisset, E. L. Brown, M. Bes, Y. Benito, E. M. Barbu, V. Vazquez, M. Höök, J. Etienne, et al. 2007. *S. aureus* Panton-Valentine leukocidin causes necrotizing pneumonia. *Science* 315: 1130–1133.
23. Sugai, M., H. Komatsuzawa, T. Akiyama, Y. M. Hong, T. Oshida, Y. Miyake, T. Yamaguchi, and H. Suginaka. 1995. Identification of endo-beta-N-acetylglucosaminidase and N-acetylmuramyl-L-alanine amidase as cluster-dispersing enzymes in *S. aureus. J. Bacteriol.* 177: 1491–1496.
24. Löffler, B., M. Hussain, M. Grundmeier, M. Brück, D. Holzinger, G. Varga, J. Roth, B. C. Kahl, R. A. Proctor, and G. Peters. 2010. *S. aureus* panton-valentine leukocidin is a very potent cytotoxic factor for human neutrophils. *PLoS Pathog.* 6: e1000715.
25. Roth, B. L., M. Poot, S. T. Yue, and P. J. Millard. 1997. Bacterial viability and antibiotic susceptibility testing with SYTOX green nucleic acid stain. *Appl. Environ. Microbiol.* 63: 2421–2431.
26. Garcia-Bermejo, M. L., F. C. Leskow, T. Fujii, Q. Wang, P. M. Blumberg, M. Ohba, T. Kuroki, K. C. Han, J. Lee, V. E. Marquez, and M. G. Kazanietz. 2002. Diacylglycerol (DAG)-lactones, a new class of protein kinase C (PKC) agonists, induce apoptosis in LNCaP prostate cancer cells by selective activation of PKCalpha. *J. Biol. Chem.* 277: 645–655.
27. Sollner-Webb, B., and G. Felsenfeld. 1975. A comparison of the digestion of nuclei and chromatin by staphylococcal nuclease. *Biochemistry* 14: 2915–2920.
28. Richmond, T. J., J. T. Finch, B. Rushton, D. Rhodes, and A. Klug. 1984. Structure of the nucleosome core particle at 7 A resolution. *Nature* 311: 532–537.
29. Kornberg, R. D., and A. Klug. 1981. The nucleosome. *Sci. Am.* 244: 52–64.
30. McGhee, J. D., and G. Felsenfeld. 1980. Nucleosome structure. *Annu. Rev. Biochem.* 49: 1115–1156.
31. Salina, D., K. Bodoor, D. M. Eckley, T. A. Schroer, J. B. Rattner, and B. Burke. 2002. Cytoplasmic dynein as a facilitator of nuclear envelope breakdown. *Cell* 108: 97–107.
32. Hirsch, J. G. 1958. Bactericidal action of histone. *J. Exp. Med.* 108: 925–944.
33. Lee, W. Y., T. J. Moriarty, C. H. Wong, H. Zhou, R. M. Strieter, N. van Rooijen, G. Chaconas, and P. Kubes. 2010. An intravascular immune response to *Borrelia burgdorferi* involves Kupffer cells and iNKT cells. *Nat. Immunol.* 11: 295–302.

34. Liu, G. Y., A. Essex, J. T. Buchanan, V. Datta, H. M. Hoffman, J. F. Bastian, J. Fierer, and V. Nizet. 2005. *S. aureus* golden pigment impairs neutrophil killing and promotes virulence through its antioxidant activity. *J. Exp. Med.* 202: 209–215.
35. Karavolos, M. H., M. J. Horsburgh, E. Ingham, and S. J. Foster. 2003. Role and regulation of the superoxide dismutases of *S. aureus. Microbiology* 149: 2749–2758.
36. Mandell, G. L. 1975. Catalase, superoxide dismutase, and virulence of *S. aureus*. In vitro and in vivo studies with emphasis on staphylococcal–leukocyte interaction. *J. Clin. Invest.* 55: 561–566.
37. Güttinger, S., E. Laurell, and U. Kutay. 2009. Orchestrating nuclear envelope disassembly and reassembly during mitosis. *Nat. Rev. Mol. Cell Biol.* 10: 178–191.
38. von Köckritz-Blickwede, M., and V. Nizet. 2009. Innate immunity turned inside-out: antimicrobial defense by phagocyte extracellular traps. *J. Mol. Med.* 87: 775–783.
39. Yost, C. C., M. J. Cody, E. S. Harris, N. L. Thornton, A. M. McInturff, M. L. Martinez, N. B. Chandler, C. K. Rodesch, K. H. Albertine, C. A. Petti, et al. 2009. Impaired neutrophil extracellular trap (NET) formation: a novel innate immune deficiency of human neonates. *Blood* 113: 6419–6427.
40. Oehmcke, S., M. Mörgelin, and H. Herwald. 2009. Activation of the human contact system on neutrophil extracellular traps. *J Innate Immun* 1: 225–230.
41. Genestier, A. L., M. C. Michallet, G. Prévost, G. Bellot, L. Chalabreysse, S. Peyrol, F. Thivolet, J. Etienne, G. Lina, F. M. Vallette, et al. 2005. *S. aureus* Panton-Valentine leukocidin directly targets mitochondria and induces Bax-independent apoptosis of human neutrophils. *J. Clin. Invest.* 115: 3117–3127.
42. Fraser, S. T., J. Isern, and M. H. Baron. 2007. Maturation and enucleation of primitive erythroblasts during mouse embryogenesis is accompanied by changes in cell-surface antigen expression. *Blood* 109: 343–352.
43. Burke, B., and C. L. Stewart. 2002. Life at the edge: the nuclear envelope and human disease. *Nat. Rev. Mol. Cell Biol.* 3: 575–585.
44. Olins, A. L., T. V. Hoang, M. Zwerger, H. Herrmann, H. Zentgraf, A. A. Noegel, I. Karakesisoglou, D. Hodzic, and D. E. Olins. 2009. The LINC-less granulocyte nucleus. *Eur. J. Cell Biol.* 88: 203–214.
45. Stewart, C. L., K. J. Roux, and B. Burke. 2007. Blurring the boundary: the nuclear envelope extends its reach. *Science* 318: 1408–1412.
46. Crisp, M., Q. Liu, K. Roux, J. B. Rattner, C. Shanahan, B. Burke, P. D. Stahl, and D. Hodzic. 2006. Coupling of the nucleus and cytoplasm: role of the LINC complex. *J. Cell Biol.* 172: 41–53.
47. Neeli, I., N. Dwivedi, S. Khan, and M. Radic. 2009. Regulation of extracellular chromatin release from neutrophils. *J Innate Immun* 1: 194–201.